Journal of Engineering Mathematics **35:** 11–42, 1999.

Ocean spray and the thermodynamics of tropical cyclones

JAMES LIGHTHILL†
Department of Mathematics, University College London, Gower Street, London WC1E 6BT, United Kingdom

Received 30 May 1997; accepted in revised form 6 April 1998

Abstract. Serious gaps in knowledge about ocean spray at wind speeds over 40m/s remain difficult to fill by observation or experiment; yet refined study of the thermodynamics of Tropical Cyclones (including typhoons and hurricanes) requires assessment of the hypothesis that 'spray cooling' at extreme wind speeds may act to reduce (i) the initial temperature of saturated air rising in the eyewall and so also (ii) the input of mechanical energy into the airflow as a whole. Such progressive reductions at higher speeds could, for example, make any possible influence of future global warming on Tropical Cyclone intensification largely self-limiting. In order to help in extrapolation of knowledge on ocean spray to extreme wind speeds, a probabilistic analysis is introduced which allows for the effects of gusts, gravity and evaporation on droplet distributions, yet in other respects is as simple as possible. Preliminary indications from this simplified analysis appear to confirm the potential importance of spray cooling.

Keywords: hurricanes, typhoons, spray, droplets, evaporation

1. The need to fill gaps in knowledge about ocean spray at extreme wind speeds

Between ocean and atmosphere there exists at high wind speeds a thick layer of 'a third fluid': ocean spray, consisting of a relatively tall cloud of droplets. Many of the smaller ones (with radii not more than about 20 μm) appear when air bubbles burst at the sea surface. A greater mass of droplets, on the other hand, is formed [1] either as 'splash' torn from, or as 'spume' ejected from, whitecaps (in the form of droplets with radii ranging from about 20 μm to much larger values).

The international project HEXOS (Humidity Exchange Over the Sea) obtained extensive data on spray over the North Sea at a '10m wind speed' (that is, mean velocity measured at height 10m above the sea surface) ranging from moderate values to not more than 18 m/s. At such speeds, little effect of spray on rates of water vapour transfer to the atmosphere was found [2].

On the other hand, the Russian research ship 'Priliv' in a 1988 Pacific cruise passed, successively, near to two typhoons, 'Tess' (8830) and 'Skip' (8831), so that data were obtained [3] at wind speeds up to 28 m/s. These were extremely careful observations, which agreed completely with HEXOS results in finding negligible effect of spray below 18 m/s; yet, at wind speeds between that value and 28 m/s, a massive increase in spray concentration was recorded. It was accompanied by a closely parallel increase, from less than 1°C to more than 5°C, in ΔT: the shortfall in air temperature below that of the sea surface. Indeed the data suggest the presence at such higher wind speeds of a 'spray cooling' phenomenon, with so much of the vapour transfer to surface winds coming from spray droplets that air heat loss to supply the requisite latent heat cannot be compensated for in full by transfer of heat from the ocean surface.

† Deceased.

Fairall, Kepert and Holland [4], in a careful study of the 'Priliv' measurements, gave a theoretical analysis in support of such a 'spray cooling' interpretation. Moreover they extended their analysis to a wind speed of 40 m/s, chosen as the speed U for which the widely used formula

$$3{\cdot}84 \times 10^{-6} U^{3{\cdot}41}, \tag{1}$$

for the fraction of sea surface [1] covered by whitecaps, reaches unity. At this speed, they predicted that the mass density of spray should reach only $0{\cdot}008\,\mathrm{kgm}^{-3}$ (less than 1% of air density) and yet that vapour transfer from spray to air should exceed direct transfer from the ocean surface by an order of magnitude.

Conclusions like theirs have great potential importance for the thermodynamics of Tropical Cyclones (including both typhoons and hurricanes). A Tropical Cyclone (TC) is an intense cyclone formed over a tropical ocean with maximum sustained winds around 50 m/s and with diameter around 1000 km. It differs from other cyclones [5] in exhibiting the famous 'eye of the storm': a central calm region – often, nearly free of clouds – surrounded by a circular 'eye-wall' consisting of exceptionally dense convective cloud.

The TC winds, that have followed long cyclonically spiralling paths over the ocean surface, become practically saturated with water vapour at the eyewall, where they are lifted to great heights by buoyancy forces (so that they never penetrate into the eye itself). This becomes possible provided that the ambient 'lapse rate' (rate of decrease of atmospheric temperature with height) is greater than the 'moist-adiabatic' lapse rate plotted in Figure 5 of [5] (this rate is very roughly 5°C per km, because the cooling of saturated air as it rises adiabatically leads to condensation and release of latent heat, reducing such cooling from the unsaturated-air rate of 10°C per km to around half that value). Then saturated air as it rises is constantly warmer than its surroundings and buoyancy can power its ascent all the way to the base of the stratosphere.

A broad view of TC thermodynamics is provided by Emanuel's heat-engine model [6], in which the working fluid is a mix of dry air with water in one or more of its forms (vapour, droplets and – at higher altitudes – ice crystals). The temperature T_1 at which the working fluid initially takes in heat (mainly, in the form of latent heat of evaporation) is to a first approximation the sea surface temperature (but see below for attempts at a second approximation). Next, an approximately adiabatic working phase (adiabatic, that is, for the moist-air working fluid) takes place in the eyewall, while a heat-loss phase occurs at a temperature T_0 characteristic of the base of the stratosphere.

Effectively, this description is that of a Carnot cycle operating between temperatures T_1 and T_0 ; which, if both temperatures are expressed in kelvins, has thermal efficiency

$$\frac{T_1 - T_0}{T_1}; \tag{2}$$

quite a substantial fraction because T_1 and T_0 have values around 300K and 200K in the tropics. The product of this efficiency (2) with heat intake per unit mass gives the input of mechanical energy per unit mass of working fluid. Such input, occurring mainly in the eyewall, must counteract that dissipation of mechanical energy per unit mass which takes place mainly in the atmospheric boundary layer at the ocean surface.

Out of the three elements in this balance, only one depends sensitively on the heat-intake temperature T_1. Turbulent dissipation per unit mass is effectively independent of temperature,

Table 1. Values taken by $100q_s(T_1, p_1)$ for $p_1 = 950$mb (a typical TC pressure).

T_1	20°C	22°C	24°C	26°C	28°C	30°C	32°C
$100q_s(T_1, p_1)$	1·52	1·73	1·95	2·19	2·47	2·77	3·10

while the Carnot efficiency (2) depends only weakly on the value of T_1. By contrast, the possible intake of latent heat per unit mass of air is proportional to $q_s(T_1, p_1)$, the saturated vapour concentration by mass for air at temperature T_1 and pressure p_1, and Table 1 shows how steeply $q_s(T_1, p_1)$ increases with T_1, by a factor of 2 as T_1 rises from 20°C to 32°C. Such critical dependence on T_1 for just this one factor in the fundamental TC energy balance suggests both

(i) why TCs are tropical phenomena (they are observed to form only when sea surface temperature is at least 26°C; and also
(ii) why the effects of spray cooling (possibly increasing in extreme winds) might act to limit TC intensities.

The latter suggestion could be particularly relevant to considerations of whether or not projected global warming is likely to enhance TC intensities – since such an enhancement, if it increased spray cooling, might become largely self-limiting (see [7] and [8]).

This paper investigates possible effects of spray distribution on T_1, defined as the average temperature at which the working fluid reaches saturation (with its full latent-heat content $L_v q_s(T_1, p_1)$ in terms of the latent L_v of water vapour) so that it can begin its buoyancy-powered rise in the eyewall. Although a first approximation to T_1 is the sea-surface temperature T_s, a thorough review of TC thermodynamics may require the use of a second approximation

$$T_1 = T_s - \Delta T. \tag{3}$$

On the other hand, it should not be assumed that the 'Priliv' measurements of sea-air temperature difference ΔT can be used in Equation (3), since all were made at a substantial distance from the eyewall of the typhoon under study. As the eyewall is approached, ΔT must be altered by two opposing effects:

(a) because the relative humidity r_H tends to 1, the cooling which a given mass of spray can produce is steadily diminished; and yet
(b) because wind speeds rise to extreme values, there may be a large increase in the mass of spray per unit horizontal area.

For applying Equation (3) to TC thermodynamics, there is a major need to fill gaps in knowledge about ocean spray at extreme wind speeds so as to be able to estimate (see Section 8 below) whether or not effect (b) on ΔT can outweigh effect (a) as the eyewall is approached.

This need has just been explained from Emanuel's heat-engine model, suggesting that the full latent heat $L_v q_s(T_1, p_1)$ which unit mass of air can acquire (with $q_s(T_1, p_1)$ given by Table 1) determines, on multiplication by a thermal efficiency (2), the mechanical energy input available for overcoming boundary-layer dissipation. Yet, even for those TC scientists who view any heat-engine model just as an interesting analogy, the critical role of T_1 must

still be evident. For them the necessary mechanical work W, done by the buoyancy force $g(\rho_a - \rho)/\rho$ which lifts unit mass of air in the eyewall (with ambient density distribution ρ_a) and which acts through a distance $\mathrm{d}z = -\mathrm{d}p/(\rho_a g)$, might be written as an integral

$$W = \int_{p_0}^{p_1} \left(\frac{1}{\rho} - \frac{1}{\rho_a} \right) \mathrm{d}p \tag{4}$$

along a moist-air adiabat, giving (from adiabatic relationships)

$$W = \int_{T_0}^{T_1} \left(c_p \, \mathrm{d}T + L \, \mathrm{d}q_s \right) - \int_{p_0}^{p_1} \frac{\mathrm{d}p}{\rho_a}. \tag{5}$$

Here, even though the latent heat L takes the value L_v (for condensation into liquid water) only in the lower part of the troposphere (condensation being to ice crystals in the upper part), the sensitivity to T_1 is again evident through the presence of a term $L_v q_s(T_1, p_1)$ in the first integral. Therefore the potential influence of ocean spray on Equation (3) for T_1 continues to be important.

Unfortunately, however, there is a serious gap in knowledge about ocean spray at extreme TC wind speeds. The 'Priliv' data extend only to 28 m/s, although a similar trend with wind speed up to 40 m/s was found by Petrichenko and Pudov [9] on analysing pre-1988 records made in the Pacific by 30 Russian research ships, and by Black, Pudov and Holland [10] on analysing records from moored buoys operated in the Gulf of Mexico by the U.S. National Data Buoy Center. Yet speeds of 50 to 60 m/s may be reached near a TC eyewall. It is this gap which needs to be filled if questions about the balance between opposing effects (a) and (b) on the value of ΔT are to be answered. On the other hand, formidable obstacles stand in the way of any efforts to derive the necessary data by direct observation of spray distributions near a TC eyewall. Accordingly, it remains hard to assess whether or not future global warming has the potential to bring about a significant increase in TC intensities.

2. Modest steps towards an improved fluid-mechanical analysis of ocean-spray distribution with height

Against the background of those serious difficulties which may oppose (see Section 1) an attempt to study ocean-spray distributions at extreme wind speeds by observation or experiment, the alternative possibility of investigation by fluid-mechanical analysis is considered in this section. Necessarily, such an essentially theoretical approach will at the best be just tentative. Indeed, all that can reasonably be attempted is to introduce some sort of supplementary analytical approach which, when used alongside approaches already available in the literature, may lead to results in which a modestly increased level of trust can be placed.

Previously existing methods range from those based [11] on the statistical theory of turbulence in the atmospheric boundary layer (HEXOS data have been fruitfully analysed by such methods) to so-called Monte Carlo simulations of droplet trajectories [12]. Here, an attempt is made to add another approach (somewhat intermediate between the two), aimed at estimating the probability distribution for the height of a particular spray droplet at various values of the time t after it first leaves the surface. This approach, designed of course for use at wind speeds far greater than those appearing in HEXOS observations, is aimed moreover at augmenting confidence, so that it may tentatively be applied, even under conditions where no comparison with observation is available.

Indeed, where models have been (very successfully) tailored towards fitting HEXOS data at North Sea wind speeds, it remains uncertain whether they are well adapted towards use at any extreme speed. For example they envisage the height of the droplet evaporation zone being closely related to significant wave height [1], which certainly leads to satisfactory agreement with HEXOS heat and vapour data – even though HEXOS measurements of actual droplet distributions [13] extended higher than the models allow for.

One objective of the present analysis is to study whether the heights of spray clouds may become much greater than has hitherto been suspected at TC wind speeds. Yet, just because of this objective (and of the need to make conclusions credible), all of those many simplifications which a practicable analysis needs to incorporate have been selected 'cautiously', in the sense that they are simplifications tending, if anything, to underestimate the heights to which spray clouds may extend.

It is especially the vertical component, w, of air velocity whose statistical properties influence (along with the effects of gravity) how droplets are vertically distributed. To a crude approximation, we may think of a parcel of air being subjected to a random succession of gusts creating different vertical movements (up or down), while a droplet within the parcel falls relatively to it under the influence of gravity at roughly its terminal velocity. This crude picture underlies the supplementary analytical approach that is introduced below.

Of course G. I. Taylor's celebrated 1921 paper 'Diffusion by continuous movements' rightly emphasized [14] how diffusion in a continuous, albeit turbulent, fluid flow differs essentially from diffusion associated with those random movements of molecules which undergo discontinuities whenever two molecules collide. For mathematically describing the effects of continuously varying random movements of a fluid particle, Taylor introduced correlation functions of the type which nowadays are generally called 'Lagrangian' (to distinguish them from the Eulerian correlation functions which later came to be used still more widely); more recently, attention was drawn by Hunt [15], as well as by subsequent authors, to the persistent value of using such functions in diffusion studies.

In an atmospheric boundary layer with statistical properties which are horizontally homogenous, the appropriate Lagrangian correlation function for characterizing random vertical displacements of a particle (small parcel) of air may be written

$$C(z,\tau) = \frac{\langle w(t)w(t+\tau)\rangle}{\left\langle [w(t)]^2 \right\rangle}. \tag{6}$$

Here, $w(t)$ represents the particle's vertical component of velocity at a certain time t when it is at height z, while $w(t+\tau)$ represents for any $\tau > 0$ the vertical component of velocity for the same particle at a later time $t+\tau$ (when in general it is at a different height); angle brackets signify an average over all such particles.

The definition (6) makes $C \to 1$ as $\tau \to 0$, while the random nature of turbulence ensures that C is effectively zero whenever τ is large. Furthermore, the integral

$$T(z) = \int_0^\infty C(z,\tau)\,\mathrm{d}\tau, \tag{7}$$

which has the dimensions of time, is often called the Lagrangian correlation time. Essentially (see Figure 1), it is a measure of that time-difference within which values of C remain significant; to a crude approximation, the correlation $C(z,\tau)$ is substantial when $\tau < T$ and yet relatively insignificant when $\tau > T$. Thus T is a sort of 'time of flight' for the coherent

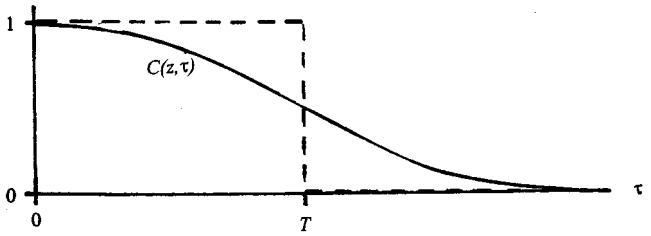

Figure 1. Solid line: typical variation of $C(z, \tau)$ with τ. Broken line: simplifying approximation.

vertical displacement of a small parcel of air, after which the immediately succeeding vertical displacement can almost be considered as if it were statistically independent. Such a view of the Lagrangian correlation time $T(z)$ may at least be more valuable than were similar views (once fashionable) about 'mixing lengths' – above all, because time is one-dimensional; whereas the three-dimensional character of space, and moreover the constraints on velocity fields provided by the equation of continuity, place obstacles in the way of any spatial analogue to the simplifying interpretation figure given in Figure 1.

The present model not only adopts this crude simplification (assuming statistically independent vertical displacements of a parcel of air in successive times of flight) but also – with the principal object of maximum simplicity – uses for the time of flight a single uniform value T independent of z. That additional simplification is made even though, in established descriptions of turbulent boundary layers over rough solid surfaces, the Lagrangian correlation time T increases with height z. Admittedly, the atmospheric boundary layer over a deeply heaving ocean surface might for small heights z above mean sea level involve increased coherence of vertical motion, which would tend to smooth out the variation of T with z; even so, the primary purpose of assuming a uniform time of flight T is to obtain a spray model simple enough to facilitate extrapolation to greatly increased wind speeds. The assumption may be 'cautious' (in the sense suggested at the beginning of Section 2) because it neglects enhanced vertical displacements experienced by droplets that have reached high levels.

Once the time of flight T has been taken independent of z, it is logical to postulate the same height-independence for a key probability distribution $g(\zeta)$ which will be called 'the gust function'. Here $g(\zeta)$ is the probability distribution for ζ, the vertical displacement of a parcel of air in the fixed time T. (Its height independence can reasonably be assumed from the fact that measured root-mean-square values for the vertical component of velocity are practically uniform across a turbulent boundary layer.) If R is the range of possible values of ζ, then the gust function $g(\zeta)$ satisfies the equations

$$\int_R g(\zeta)\,\mathrm{d}\zeta = 1, \qquad \int_R \zeta g(\zeta)\,\mathrm{d}\zeta = 0, \qquad \int_R \zeta^2 g(\zeta)\,\mathrm{d}\zeta = G, \tag{8}$$

for a probability distribution with zero mean and with variance G. In what follows, $g(\zeta)$ will normally be taken as an even function with range $|\zeta| < Z$.

This paper's primary concern is to estimate $f(z, t)$, the probability distribution for the height z of a spray droplet at time t after leaving the level $z = 0$. During the time of flight T a droplet within a parcel of air descends relatively to it by a distance close to VT, where V is its terminal velocity (at least, on a 'cautious' assumption that ignores any possible levitating

influence of such coherent eddy motions as may help to keep droplets aloft in rainclouds). This implies that $f(z,t)$ satisfies the integro-difference equation

$$f(z - VT,\ t + T) = \int_R f(z - \zeta, t) g(\zeta)\, \mathrm{d}\zeta, \tag{9}$$

where the right-hand convolution of the probability distribution for the droplet being at height $z - \zeta$ at time t with the probability of the parcel of air being displaced by ζ during the time of flight T gives the probability distribution for the parcel being at height z, and so also for the droplet being at height $z - VT$, at time $t + T$. (Here, with expected mass densities for droplets [4] of order 10^{-2} corresponding to volume densities of order 10^{-5}, interaction between droplets may reasonably be neglected.)

Evidently, the initial condition appropriate to solutions of this integro-difference equation is

$$f(z, 0) = \delta(z) \tag{10}$$

because the probability distribution $f(z,t)$ by its definition is concentrated at just one value $z = 0$ at time $t = 0$. The boundary condition, on the other hand, needs more careful consideration.

Essentially, this boundary condition must take into account the fact that the life of a spray droplet cannot continue after it has once returned to the ocean surface. Admittedly, that surface's height changes continually; here, however, the cautious assumption is made that a droplet disappears as soon as it has regained its initial height; in other words, when z becomes zero. This assumption may be described as cautious (erring on the side of over-predicting the reabsorption of spray droplets) simply because the majority of droplets are believed to be generated at levels higher than mean ocean-surface levels. For applying such a boundary condition to the integro-difference equation (9), it is sufficient to specify (as an overriding requirement) that

$$f(z,t) = 0 \text{ for all } z < 0. \tag{11}$$

This excludes from the range of integration R all values of ζ greater than z; while, still more simply, it requires Equation (9) to be ignored whenever $z < VT$.

In the next two sections, exact solutions of Equation (9) under conditions (10) and (11) are compared with exact solutions of a partial differential derived from it by an approximation scheme of Fokker–Planck type. In this scheme, the expression $f(z - \zeta, t)$ is approximated as just the first three terms of its Taylor series, to make the right-hand side

$$\int_R \left[f(z,t) - \zeta \frac{\partial f}{\partial z} + \frac{1}{2}\zeta^2 \frac{\partial^2 f}{\partial z^2} \right] g(\zeta)\, \mathrm{d}\zeta, \tag{12}$$

which by Equation (8) is

$$f(z,t) + \frac{1}{2} G \frac{\partial^2 f}{\partial z^2}. \tag{13}$$

The left-hand side is then approximated as

$$f(z,t) + T\left(\frac{\partial f}{\partial t} - V \frac{\partial f}{\partial z} \right) \tag{14}$$

to yield a partial differential equation of convection-diffusion type,

$$\frac{\partial f}{\partial t} - V\frac{\partial f}{\partial z} = D\frac{\partial^2 f}{\partial z^2}, \quad \text{where } D = \frac{G}{2T} \tag{15}$$

is the diffusivity. In the 'comparison' Section 4, appropriate solutions of Equation (15) are found to represent solutions of (9) in an asymptotic sense, with quite reasonable accuracy achieved already for surprisingly modest values of t/T.

3. Solutions of the integro-difference equation for a particular case

In a first attempt to make such a comparison, the particular form chosen for the function $g(\zeta)$ was the simple piecewise-constant form

$$g(\zeta) = \tfrac{1}{2}Z^{-1} \text{ for } -Z < \zeta < Z \quad \text{and} \quad = 0 \text{ for } |\zeta| > Z, \tag{16}$$

which satisfies Equations (8) with G taking the uniform value

$$G = \tfrac{1}{3}Z^2. \tag{17}$$

Evidently, just because the discontinuous form of g leads to solutions for f with discontinuities in its gradient $\partial f/\partial z$, the test of whether such solutions asymptotically resemble those of the partial differential equation (15) becomes quite an exacting one.

The physical problem described by the above choice is something of a classical 'random walk'. During each time interval T a small parcel of air is subjected to a random gust which gives it a vertical displacement taking any value from $-Z$ to $+Z$ with equal probability, while a droplet within that parcel of air descends by a distance VT relative to it. Clearly, the nature of solutions must depend critically on the ratio of VT to Z. This may be designated as

$$\frac{VT}{Z} = \varepsilon, \tag{18}$$

where the letter ε is used because the most interesting distributions of ocean spray, appropriate to extreme-wind conditions, are expected to be those where the range Z of vertical displacements by gusts is much bigger than a simultaneous downward displacement VT of a droplet by gravity. Nonetheless it must be stressed that the problem defined above is solved here for arbitrary values of ε – without any approximation for small ε being required.

The integro-difference equation (9), subject to the boundary condition (11), which excludes from the range of integration R all values of ζ greater than z, can be regarded as a recurrence formula determining functions $f_n(x)$ defined as

$$f_n(x) = Zf(Zx, nT) \text{ where } x \geqslant 0 \tag{19}$$

for successive positive integers n. After a further substitution $\zeta = Z\xi$ in the integral, Equation (9) becomes

$$f_{n+1}(x - \varepsilon) = \tfrac{1}{2}\int f_n(x - \xi)\,\mathrm{d}\xi, \tag{20}$$

taken over the range of integration $|\xi| < 1,\ x - \xi > 0$. Finally, with y replacing $x + \varepsilon - \xi$, we obtain

$$f_{n+1}(x) = \tfrac{1}{2}\int_N f_n(y)\,\mathrm{d}y, \tag{21}$$

where the new range N is defined by the inequalities

$$y > 0,\ \ -1 < y - x - \varepsilon < 1. \tag{22}$$

The recurrence formula (21) defines uniquely all the distributions $f_n(x)$ for $n \geqslant 0$ given the initial condition

$$f_0(x) = Zf(Zx, 0) = Z\delta(Zx) = \delta(x) \tag{23}$$

specified by Equation (10). In particular, $f_1(x)$ is the step function

$$f_1(x) = \tfrac{1}{2}\ (0 < x < 1 - \varepsilon),\ \ 0\ (1 - \varepsilon < x), \tag{24}$$

after which classical integral calculus allows every subsequent $f_n(x)$ to be determined. For example, $4f_2(x)$ takes the values

$$1 - \varepsilon,\ \ 2 - 2\varepsilon - x \text{ and } 0 \tag{25}$$

in the intervals $0 < x < 1 - \varepsilon,\ \ 1 - \varepsilon < x < 2 - 2\varepsilon$ and $2 - 2\varepsilon < x$, respectively. Similarly, $8f_3(x)$ for $x > 0$ takes the values

$$1 - 3\varepsilon^2 + (1 - 3\varepsilon)x - \tfrac{1}{2}x^2,\ \ \tfrac{3}{2}(1 - \varepsilon)^2,$$

$$\tfrac{5}{2}(1 - \varepsilon)^2 - (1 - \varepsilon)x,\ \ \tfrac{1}{2}(3 - 3\varepsilon - x)^2 \text{ and } 0 \tag{26}$$

in intervals separated by the points $x = 1 - 3\varepsilon,\ \ 1 - \varepsilon,\ \ 2 - 2\varepsilon$ and $3 - 3\varepsilon$.

The distributions $f_4(x)$ and $f_5(x)$ are somewhat more complicated. Thus, $16f_4(x)$ takes values for $x > 0$ given by quite different algebraic expressions in intervals separated by the points $x = 1 - 3\varepsilon,\ \ 1 - \varepsilon,\ \ 2 - 4\varepsilon,\ \ 2 - 2\varepsilon$ and $3 - 5\varepsilon$; out of which, in order to save space, while still allowing verification by the reader, only the first and last are quoted here:

$$\tfrac{4}{3} - 8\varepsilon^2 + 8\varepsilon^3 + \left(\tfrac{3}{2} - 5\varepsilon + \tfrac{7}{2}\varepsilon^2\right)x - \tfrac{1}{2}(1 - \varepsilon)x^2 \tag{27}$$

and

$$\tfrac{1}{6}(4 - 4\varepsilon - x)^3 H(4 - 4\varepsilon - x) - \tfrac{1}{6}(3 - 3\varepsilon - x)^3 H(3 - 3\varepsilon - x), \tag{28}$$

where H is the Heaviside function (1 for positive, and 0 for negative, values of its argument). Furthermore, $32f_5(x)$ takes values for $x > 0$ given by different expressions in intervals separated by the points $x = 1 - 5\varepsilon,\ \ 1 - 3\varepsilon,\ \ 1 - \varepsilon,\ \ 2 - 4\varepsilon,\ \ 2 - 2\varepsilon$ and $3 - 5\varepsilon$; the first and last now being

$$\tfrac{23}{12} - \tfrac{25}{2}\varepsilon^2 + \tfrac{125}{4}\varepsilon^4 + \left(\tfrac{7}{3} - 6\varepsilon - 11\varepsilon^2 + 36\varepsilon^3\right)x$$

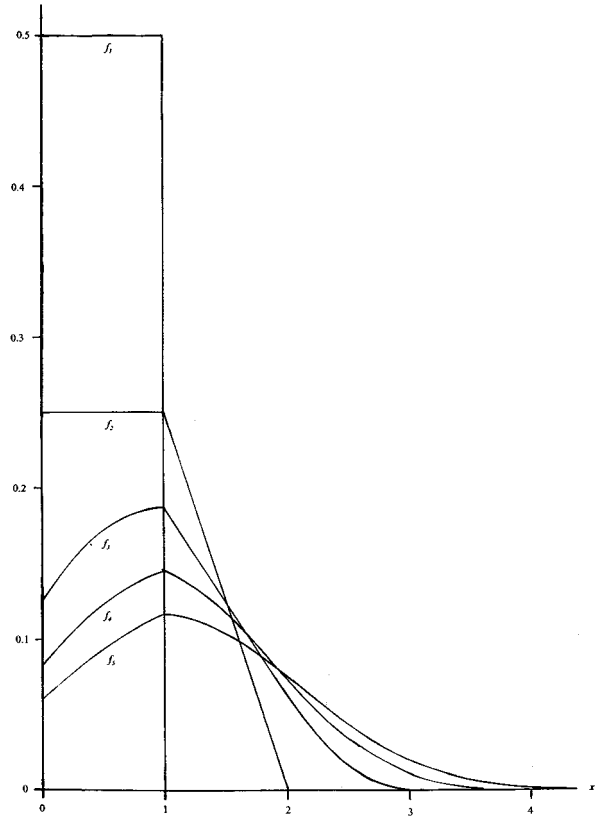

Figure 2. The functions $f_n(x)$ plotted against x for $n = 1$ to 5 in the case $\varepsilon = 0$.

$$+\left(-\tfrac{1}{4}-\tfrac{7}{2}\varepsilon+\tfrac{47}{4}\varepsilon^2\right)x^2+\left(-\tfrac{1}{3}+\tfrac{5}{3}\varepsilon\right)x^3+\tfrac{1}{12}x^4 \tag{29}$$

and

$$\begin{aligned}\tfrac{1}{24}(5-5\varepsilon-x)^4\,H\,(5-5\varepsilon-x)\;-\;\tfrac{1}{24}(4-4\varepsilon-x)^4\,H(4-4\varepsilon-x)\\ -\tfrac{1}{6}(1-\varepsilon)(3-3\varepsilon-x)^3H(3-3\varepsilon-x),\end{aligned} \tag{30}$$

respectively. Needless to say, the most comprehensive checks on the correctness of all the algebraic expressions calculated for $f_n(x)$ with $n = 1$ to 5 have been made.

Far more important, however, than these algebraic expressions are the actual values of the functions $f_n(x)$, as plotted in Figures 2 to 6. Here, Figure 2 for the special case $\varepsilon = 0$ shows all five functions plotted to the same scale to give a clear view of their relative magnitudes; while, on the other hand, each $f_n(x)$ for $2 \leqslant n \leqslant 5$ is plotted in Figures 3 to 6 for five different values (0, 0·05, 0·1, 0·15 and 0·2) of ε, with different scales used in each figure so as to offer for each n as much detailed information as possible.

4. Comparisons with relevant solutions of the partial differential equation

In Section 3 exact solutions of the integro-difference Equation (9) were derived, and plotted in Figures 2 to 6, for the particular case specified at the beginning of that section. Now those

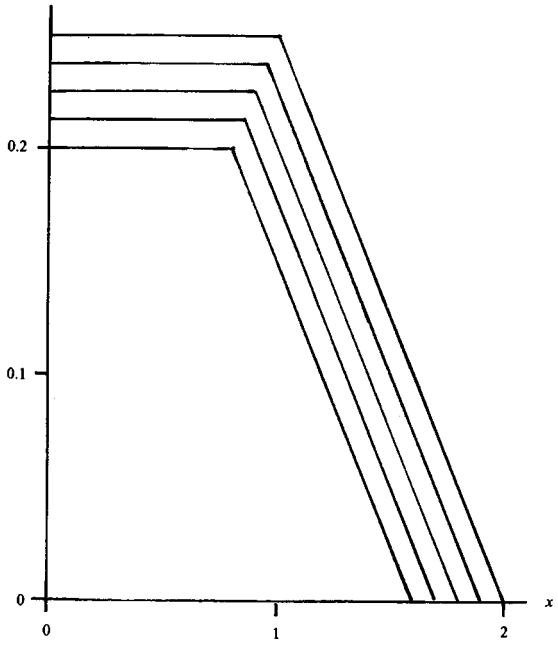

Figure 3. Plots of $f_2(x)$ for five values of ε (namely, 0, 0·05, 0·1, 0·15 and 0·2, reading from top to bottom).

solutions are given asymptotic interpretations for relatively large values of t in terms of elementary solutions of the partial differential equation (15). Such interpretations are presented first for the curves of Figure 2, representing the limiting case $\varepsilon = 0-$ an important limit because, in extreme winds, values of ε are expected to be small for most droplets.

The recurrence formula (21) might be thought to suggest a halving of magnitude of each $f_{n+1}(x)$ with respect to $f_n(x)$; yet Figure 2 shows that, except in the case $n = 1$, the magnitude as measured by both boundary and maximum values,

$$b_n = f_n(0) \text{ and } m_n = \max_{x \geqslant 0} f_n(x), \tag{31}$$

falls a lot more slowly with n. Also, reduced magnitude is accompanied by increased range, so that the integral

$$I_n = \int_0^\infty f_n(x)\,\mathrm{d}x, \tag{32}$$

representing the overall probability that a droplet remains unabsorbed, falls more slowly still. Moreover, the moment

$$M_n = \int_0^\infty x f_n(x)\,\mathrm{d}x = X_n I_n \tag{33}$$

of the probability distributions does not fall at all, while the ratio $X_n = M_n/I_n$, giving the mean height of unabsorbed droplets, steadily increases.

Log-log plots of all the above quantities against n, shown in Figure 7, are consistent in each case with an asymptotic power-law behaviour given by one of the straight lines. These represent (i) limiting forms

$$b_n \sim 0{\cdot}68n^{-3/2}, \qquad m_n \sim 0{\cdot}59n^{-1} \quad \text{and} \quad I_n \sim 0{\cdot}56n^{-1/2}, \tag{34}$$

towards which the exactly determined points plotted for $n = 2, 3, 4$ and 5 appear to converge rapidly, and (ii) asymptotes (identifiable to just one significant figure)

$$2M_n \to 0{\cdot}8 \quad \text{and} \quad X_n \sim 0{\cdot}7n^{1/2}, \tag{35}$$

towards which the exact points seem to be tending as n increases – although each of the five quantities $b_n,\ m_n,\ I_n,\ 2M_n$ and X_n plotted in Figure 7 starts out for $n = 1$ from the same value 0·5 shown there as a ringed point.

Actually, the third coefficient 0·56 in the asymptotic expressions (34) is written from now on as $\pi^{-1/2}$ to which it is extremely close; indeed, for $1 \leqslant n \leqslant 5$, and despite the complexity of expressions for $f_n(x)$ in different intervals of x, the integral (32) simplifies to

$$I_n = \frac{1.3.5 \ldots (2n-1)}{2.4.6 \ldots (2n)}, \tag{36}$$

which is asymptotically $(\pi n)^{-1/2}$ for large n. Then Equation (19) gives

$$\int_0^\infty f(z,t)\,\mathrm{d}z \sim \left(\frac{T}{\pi t}\right)^{1/2} \tag{37}$$

for large t.

Such asymptotic tendencies may now be related to solutions of the partial differential equation (15) which, in the simple case when G takes the value (17) and when $\varepsilon = 0$ (so that Equation (18) gives $V = 0$), becomes the classical diffusion equation

$$\frac{\partial f}{\partial t} = D\frac{\partial^2 f}{\partial z^2} \text{ with diffusivity } D = \frac{Z^2}{6T}. \tag{38}$$

A standard solution which satisfies the initial condition (10), although it has zero diffusive transport $D\partial f/\partial z$ across $z = 0$, is the Gaussian probability distribution

$$f_G(z,t) = \frac{1}{2(\pi Dt)^{1/2}}\,\mathrm{e}^{-\frac{z^2}{4Dt}}, \tag{39}$$

with the expected increase in range like $(Dt)^{1/2}$. Yet, f_G has a constant integral rather than one showing the asymptotic decrease (37). On the other hand, its z-derivative has an integral from 0 to ∞ equal to $-f_G(0,t)$, so that condition (37) is satisfied by $\partial f_G/\partial z$ if multiplied by a suitable constant to yield

$$f(z,t) = -2(DT)^{1/2}\frac{\partial f_G}{\partial z} = \left(\frac{T}{\pi t}\right)^{1/2}\frac{z}{2Dt}\,\mathrm{e}^{-\frac{z^2}{4Dt}}. \tag{40}$$

Then Equation (19), with the value (38) for D, gives

$$f_n(x) = \left(\frac{1}{\pi n}\right)^{1/2}\frac{3x}{n}\,\mathrm{e}^{-\frac{3x^2}{2n}}; \tag{41}$$

which agrees with two of the limiting forms (34) since, besides having $I_n = 0{\cdot}56n^{-1/2}$, it has maximum value

$$m_n = \left(\frac{3}{\pi e}\right)^{1/2} n^{-1} = 0{\cdot}59n^{-1}, \tag{42}$$

attained for $x = (n/3)^{1/2}$. Also, it is consistent with the asymptotes (29), since it gives

$$M_n = \int_0^\infty x f_n(x)\,\mathrm{d}x = 6^{-1/2} = 0{\cdot}408 \tag{43}$$

and $X_n = M_n/I_n = 0{\cdot}724n^{1/2}$.

Thus, Equation (37) may in a crude sense represent an ultimate asymptotic form for $f_n(x)$; nevertheless, it suffers from at least three unsatisfactory features:

(a) it has zero boundary value $b_n = f_n(0)$, unlike the true solutions of the integro-difference equation (21) as plotted in Figure 2;
(b) its maximum (42) is reached where x has the unrealistically high value $(n/3)^{1/2}$; and
(c) the moment M_n remains fixed at its asymptotically constant value (43) instead of rising towards it gradually as n increases.

Every one of these disadvantages may be overcome by a quite small shift in the origin of x; say, to $x = -a$ (this implies a change in the origin of z to $z = -aZ$, permissible since $f(z + aZ, t)$ is a solution of Equation (38) whenever $f(z, t)$ is).

After such a revision of expression (41) to

$$f_n(x) = \left(\frac{1}{\pi n}\right)^{1/2} \frac{3(x+a)}{n}\,\mathrm{e}^{-\frac{3(x+a)^2}{2n}}, \tag{44}$$

the above unsatisfactory features are seen to disappear. Thus, $f_n(x)$ takes a value

$$b_n = \left(\frac{1}{\pi n}\right)^{1/2} \frac{3a}{n} \tag{45}$$

at $x = 0$, while its peak value (42) is unchanged but is attained for

$$x = \left(\frac{n}{3}\right)^{1/2} - a. \tag{46}$$

Moreover, the integral I_n undergoes only a minor change to

$$\left(\frac{1}{\pi n}\right)^{1/2} \mathrm{e}^{-\frac{3a^2}{2n}} \tag{47}$$

which remains very close to $(\pi n)^{-1/2}$ for small a, when, however, M_n receives a more substantial change to

$$6^{-1/2} - a(\pi n)^{-1/2}. \tag{48}$$

Expression (48) for M_n strongly suggests the choice $a = 0{\cdot}30$, since exactly calculated values for $(6^{-1/2} - M_n)(\pi n)^{1/2}$ are 0·280, 0·292, 0·294, 0·295 and 0·296 for $n = 1, 2, 3, 4$ and 5. This choice 0·30 for a is indeed small enough for the exponential in (47) to be very near 1 for the larger values of n.

A slightly higher estimate for a is indicated by Equation (45) which, while agreeing with results obtained earlier in making b_n proportional to $n^{-3/2}$, allows the coefficients in (45) and (34) to coincide only if $a = 0{\cdot}40$. There are, however, good reasons for giving more weight to

the choice $a = 0{\cdot}30$, derived from an integral property (33) of the distribution (its moment), than to the choice $a = 0{\cdot}40$ inferred from a single value $b_n = f_n(0)$. First of all, M_n is preferentially affected by values of $f_n(x)$ for larger x (representing the distribution of spray away from the surface) which are the values of primary interest. Furthermore, a distribution (44) with continuous slope must mainly be considered appropriate for approximating that part of the curve of $f_n(x)$ which has continuous slope; namely, the part with $x > 1$. If so, then expression (46) needs to be interpreted as that value of x for which the curve representing $f_n(x)$ for $x > 1$ would reach its maximum if extrapolated back to $x < 1$. For the exact f_4 and f_5 curves shown in Figure 2 this happens for $x = 0{\cdot}775$ and $x = 0{\cdot}945$ respectively – while Equation (46) after the choice $a = \frac{1}{3}$ (which attaches twice as much weight to $0{\cdot}30$ as to $0{\cdot}40$) would give the reasonably close values $x = 0{\cdot}822$ and $x = 0{\cdot}958$.

The above considerations, all taken together, suggest that a good asymptotic approximation to $f_n(x)$ may be given by Equation (44) with

$$a = \tfrac{1}{3}. \tag{49}$$

This suggestion is also supported by Figure 8, where the exact f_4 and f_5 curves, despite their discontinuities of slope at $x = 1$, are shown to be numerically close to their smoothed approximations (44). (Here, the functions plotted are $f_4(x)$ and $2f_5(x)$ in order that one diagram can, with no confusing overlap, show both curves – which, furthermore, have heights as in Figures 5 and 6, respectively.)

A solution of the diffusion equation (38) that asymptotically represents solutions of the integro-difference equation is given then, from Equations (19) and (44), as

$$f(z,t) = \left(\frac{T}{\pi t}\right)^{1/2} \frac{z + aZ}{2Dt}\, \mathrm{e}^{-\frac{(z+aZ)^2}{4Dt}}. \tag{50}$$

This asymptotic solution satisfies a more complicated boundary condition than the simple solutions (40) and (39); for which, respectively, $f = 0$ and $\partial f/\partial z = 0$ on $z = 0$. Asymptotically, the solution (50) satisfies

$$f = aZ\frac{\partial f}{\partial z} \quad \text{on} \quad z = 0, \tag{51}$$

and it is worth considering how this boundary condition, with the value (49) for a, should be interpreted.

The true boundary condition, stating (Section 3) that 'a droplet disappears as soon as it has regained its initial height' (that is, $z = 0$), may on the basis of the diffusion equation (38) be viewed as a statement about the rate $D\partial f/\partial z$ of diffusive transport into the surface at $z = 0$. During a single time of flight T, Equation (16) allows the vertical displacement of a droplet to take all values between $-Z$ and Z with equal probability, and so the chance of a droplet initially at height $z < Z$ reaching $z = 0$ is $(Z - z)/2Z$. Therefore

$$TD\left(\frac{\partial f}{\partial z}\right)_{z=0} = \frac{1}{2Z}\int_0^Z (Z - z)\, f(z,t)\, \mathrm{d}z, \tag{52}$$

a boundary condition relating total diffusive transport during time T to the distribution $f(z,t)$ of droplets at heights $z < Z$. Now, if we approximate, the right-hand side, using just two terms of a Taylor series as

$$\frac{1}{2Z}\int_0^Z (Z - z)\left[f(0,t) + z\left(\frac{\partial f}{\partial z}\right)_{z=0}\right]\mathrm{d}z, \tag{53}$$

then Equation (52) with expression (38) for D gives

$$\tfrac{1}{6}Z^2\left(\frac{\partial f}{\partial z}\right)_{z=0} = \tfrac{1}{4}Zf(0,t) + \tfrac{1}{12}Z^2\left(\frac{\partial f}{\partial z}\right)_{z=0}, \tag{54}$$

which indeed yields the simple boundary condition (51) with $a = \frac{1}{3}$, as satisfied by the asymptotic representation (50) of exact solutions of the integro-difference equation.

It must, of course, be emphasized that the amplitude of any such form (50) for relatively large t cannot be deductively related to initial conditions at $t = 0$. Nonetheless, after the asymptotic boundary condition (51) has come into force, any solution of the diffusion equation (38) can easily be proved to maintain constant values of the integral

$$\int_0^\infty (z + aZ)\, f(z)\, \mathrm{d}z, \tag{55}$$

which, moreover, takes for the representation (50) the asymptotically constant value

$$6^{-1/2}Z = 0{\cdot}408Z \tag{56}$$

(corresponding to the value $6^{-1/2}$ given by Equation (48) for $M_n + aI_n$). At least expression (56) is of broadly similar magnitude to the value of the integral (55) for $t = 0$, given by Equation (10) as

$$aZ = 0{\cdot}333Z, \tag{57}$$

and this may add just a little to existing confidence in the asymptotic representation (50) – even though no means is available for predicting the exact amplitude of such an asymptotic form.

The above extended discussion of the limiting case $\varepsilon = 0$ provides solid foundations for a far briefer account of cases with $\varepsilon > 0$. Then the partial differential equation (15) is the convection-diffusion equation, of which an exact solution closely analogous to (50) may be written

$$f(z,t) = B(\varepsilon)\left(\frac{T}{\pi t}\right)^{1/2}\frac{z + aZ}{2Dt}\,\mathrm{e}^{-\frac{(z+Vt+aZ)^2}{4Dt}}. \tag{58}$$

Here a multiplying factor $B(\varepsilon)$, for which $B(0) = 1$, has been included to allow for the above-noted uncertainties regarding amplitudes of asymptotic forms. The corresponding revision to Equation (44) for $f_n(x)$ is

$$f_n(x) = B(\varepsilon)\left(\frac{1}{\pi n}\right)^{1/2}\frac{3(x+a)}{n}\,\mathrm{e}^{-\frac{3(x+\varepsilon n+a)^2}{2n}}. \tag{59}$$

The main motivation for seeking a solution (58) of Equation (15) which, in comparison with its form (50) for $\varepsilon = 0$, involves a simple shift (from z to $z + Vt$) within the exponent, arises from the study of Figures 4, 5 and 6 for $f_3(x)$, $f_4(x)$ and $f_5(x)$. In the far right-hand parts of these figures, every curve for $\varepsilon > 0$ appears to be shifted to the left by approximately a distance εn from the curve for $\varepsilon = 0$, and expression (59) has just this property because it is

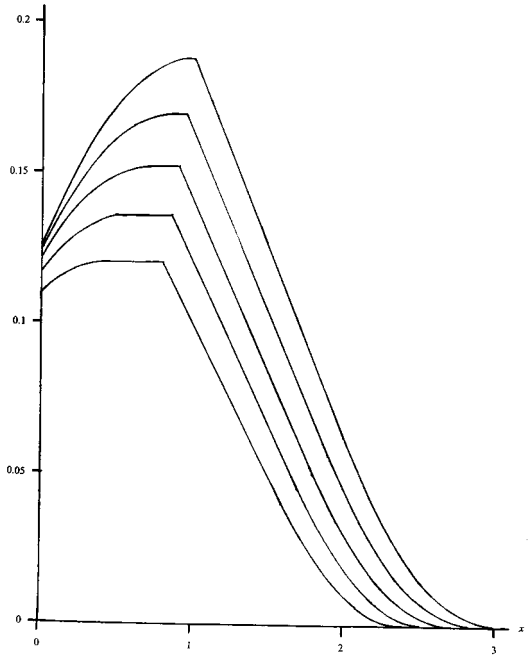

Figure 4. Similar plots of $f_3(x)$.

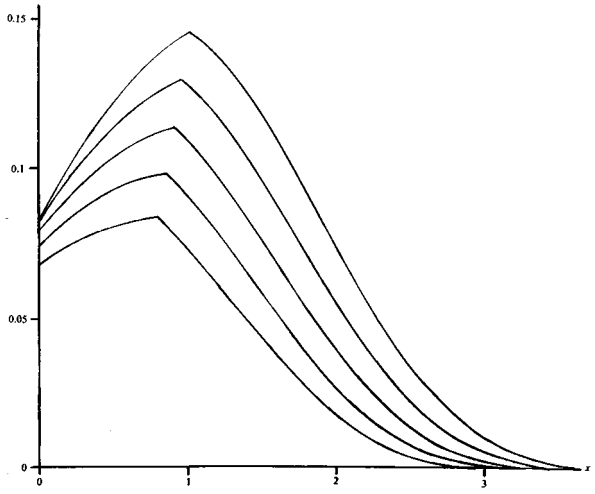

Figure 5. Similar plots of $f_4(x)$.

for the larger values of x that changes in the exponential dominate over changes in the factor outside it.

Figure 9 shows moreover that the asymptotic form (59), with

$$B(\varepsilon) = 1 + 1{\cdot}6\varepsilon, \quad a = \tfrac{1}{3}, \tag{60}$$

gives just as close a representation of the f_4 and f_5 curves for $\varepsilon > 0$ as was found in Figure 8 for $\varepsilon = 0$. Here it is interesting to note that such closeness of representation makes no requirement on a to vary with ε, even though the amplitude factor needs to be allowed a modest variation (from 1·00 to 1·32 as ε increases from 0 to 0·20). Once again, overlap between

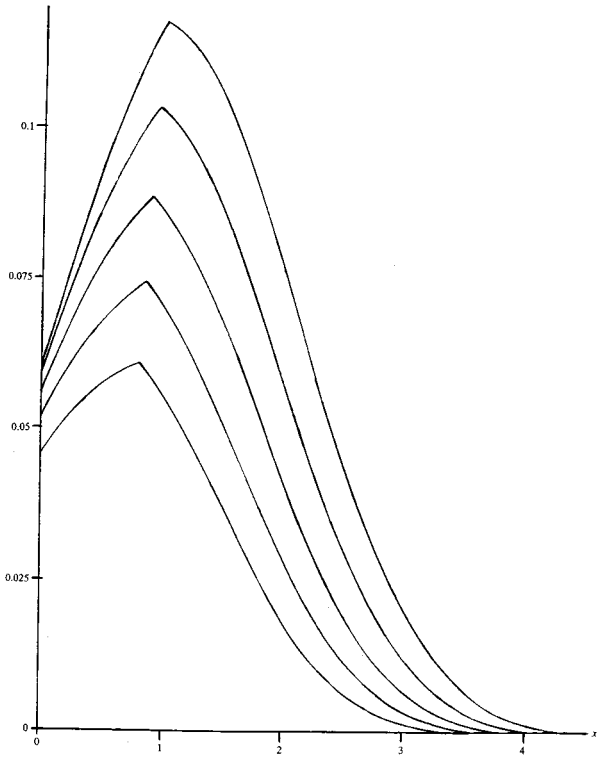

Figure 6. Similar plots of $f_5(x)$.

curves in Figure 9 is avoided by plotting $f_4(x)$ and $2f_5(x)$; while, for further avoidance of overlap, the curves for $\varepsilon = 0{\cdot}05$ and $\varepsilon = 0{\cdot}15$ are omitted in the former case, and those for $\varepsilon = 0{\cdot}10$ and $\varepsilon = 0{\cdot}20$ in the latter, even though agreement with the asymptotic form (59) is equally good for those curves which have been omitted.

Under conditions (60), then, the solution (58) of the partial differential equation (15) gives an asymptotic representation of solutions of the integro-difference equation (9) which offers reasonable accuracy after just 4 or 5 times of flight. This conclusion for a case when the gust function g takes the discontinuous form (16) is particularly encouraging because, despite consequent discontinuities in slope in solutions of the integro-difference equation, these are quite well represented by the asymptotic form (58) with continuous slope. Similar agreement is evidently still likelier when g has a smooth form; and, as a first step, Section 5 offers an extension to cases when $g(\zeta)$ takes a rather general continuous form as function of ζ.

5. Some initial steps towards generalisation

Before attempting such a natural generalisation, however, it may be worth pausing to consider, in the very simple case (16), what implications the conclusions of Section 4 would have for the spatial distribution of spray droplets. It is indeed the somewhat dramatic nature of those implications which acts as a spur to seeking out more general conclusions.

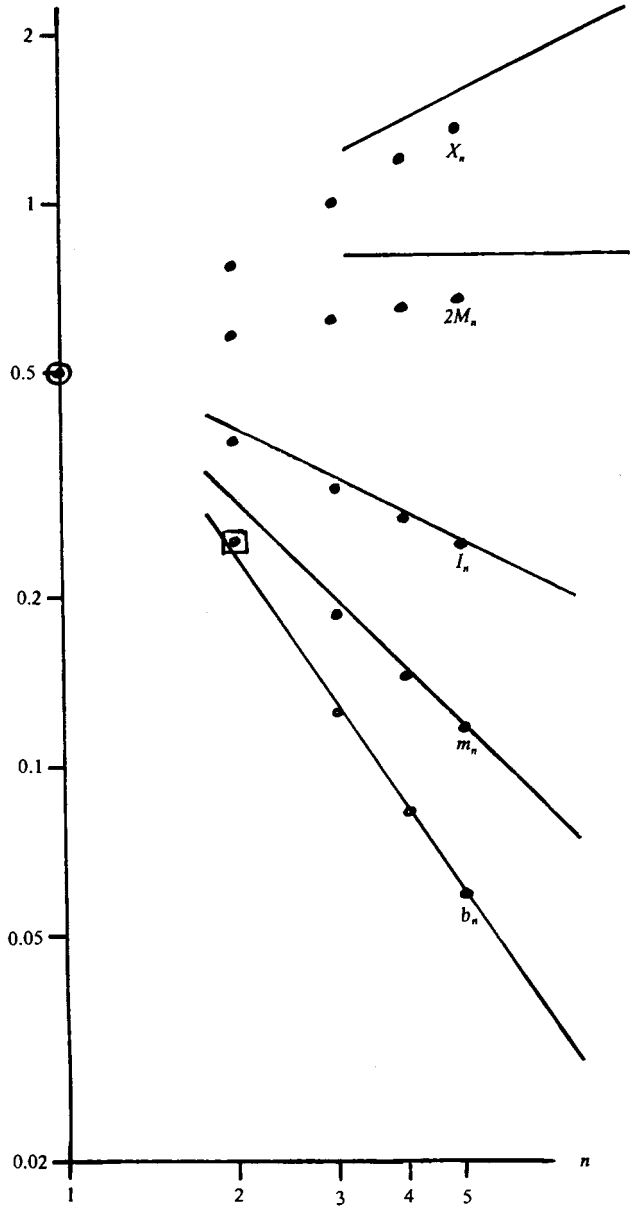

Figure 7. Log-log plots of $b_n, m_n, I_n, 2M_n$ and X_n against n for $n = 1$ to 5 (all take the ringed value 0·5 for $n = 1$, while the square marks a common value $b_2 = m_2 = 0{\cdot}25$), shown alongside the asymptotes (34) and (35).

The definition of $f(z, t)$ – as a probability distribution for the height z of a spray droplet at time t after it first appears at $z = 0$ – implies a rather special meaning for the integral

$$F(z) = \int_0^\infty f(z, t)\,\mathrm{d}t. \tag{61}$$

Very briefly, if at all times the surface $z = 0$ behaved as a source generating droplets at an average rate S per unit area per unit time, then $Sf(z, t)\,\mathrm{d}t$ would at any instant be the volume distribution at height z of droplets which had been generated at times between t and $t + \mathrm{d}t$

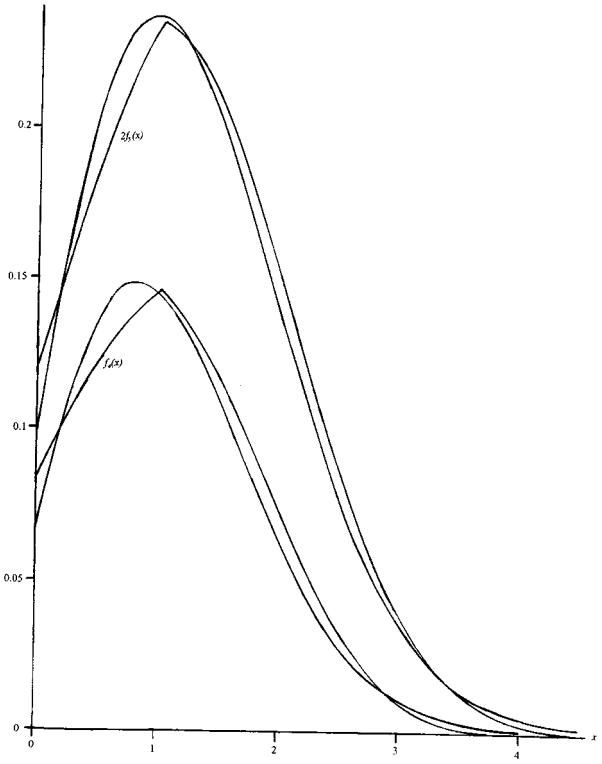

Figure 8. Comparisons, when $\varepsilon = 0$, of exact (kinked) curves for $f_4(x)$ and $2f_5(x)$ with their (smooth) asymptotic forms (44).

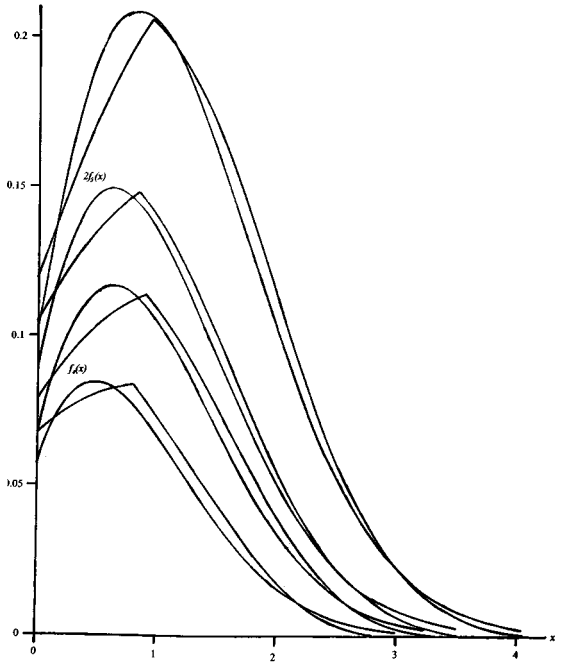

Figure 9. Comparisons of exact (kinked) curves for $f_4(x)$ with $\varepsilon = 0{\cdot}1$ and $\varepsilon = 0{\cdot}2$, and for $2f_5(x)$ with $\varepsilon = 0{\cdot}05$ and $\varepsilon = 0{\cdot}15$, with their (smooth) asymptotic forms (59).

earlier on; therefore, the volume distribution of all the droplets generated at previous times would be $SF(z)$. The true situation, however, is a little more complicated because the form of $f(z,t)$ depends on the terminal velocity V. Thus, it is necessary to define a source function $S(V)\,\mathrm{d}V$ as the rate of production per unit area per unit time of droplets having terminal velocities between V and $V+\mathrm{d}V$ (see [1] for a compendium of existing knowledge on source functions) in order that

$$[S(V)\,\mathrm{d}V]F(z) \tag{62}$$

may represent the volume distribution of such droplets at height z.

The most dramatic deduction from Section 4 is the form of $F(z)$ for $V=0$ at relatively large heights; say, for $z>3Z$ (or $x>3$). Then f_1, f_2 and f_3 vanish (Figure 2) so that all contributions to the integral (61) are from $n\geqslant 4$; that is, from times $t\geqslant 4T$ for which the asymptotic representation (50) may be used in the integral. Then, after the substitutions

$$\tau=\frac{(z+aZ)^2}{4Dt},\qquad \mathrm{d}\tau=-\frac{(z+aZ)^2}{4Dt^2}\,\mathrm{d}t, \tag{63}$$

the integral (61) becomes

$$F(z)=\left(\frac{T}{\pi D}\right)^{1/2}\int_0^\infty \tau^{-1/2}\,\mathrm{e}^{-\tau}\,\mathrm{d}\tau=\left(\frac{T}{D}\right)^{1/2}=\frac{T}{Z}6^{1/2}, \tag{64}$$

a value independent of z. In brief summary, diffusion by random gusts can, given time, raise weightless droplets to arbitrary heights – notwithstanding the fact that any which return to the surface are reabsorbed. (Note: swifts are commonly observed in strong winds feeding at heights exceeding 1 km on the aeroplankton of insects which remains abundant at such heights.)

It could be argued, of course, that, whenever the infinite integral (61) converges (as it does when f takes the form (50), even though for (39) it diverges), then $F(z)$ must be a time-independent solution of Equation (38); that is, either a linear function of z or else a still simpler constant function such as has been found. No argument along these lines, however, could predict the value (64) of that constant – which usefully equates the volume distribution of weightless droplets to their production per unit area in a single time of flight T, multiplied by $6^{1/2}Z^{-1}$. (As before, there exists no easy route to inferring amplitude.)

Yet prime interest is attached, not to weightless droplets, but to those with a positive – albeit small – terminal velocity V. Then Equations (24), (25) and (26) confirm that (once again) f_1, f_2 and f_3 vanish for $z\geqslant 3Z$; where, therefore, $f(z,t)$ can be represented by its asymptotic form (58). Here the exponential factor may, after the substitution (63), be written

$$\mathrm{e}^{-\left(\tau+\eta+\frac{\eta^2}{4\tau}\right)}\quad\text{with}\quad \eta=\frac{V(z+aZ)}{2D}, \tag{65}$$

so that the integral (61) becomes

$$F(z)=B(\varepsilon)\left(\frac{T}{\pi D}\right)^{1/2}\mathrm{e}^{-\eta}\left[\int_0^\infty \tau^{-1/2}\,\mathrm{e}^{-\left(\tau+\frac{\eta^2}{4\tau}\right)}\,\mathrm{d}\tau\right]. \tag{66}$$

The square brackets in (66) enclose a standard integral from Bessel-function theory, equal to $\pi^{1/2}\,\mathrm{e}^{-\eta}$; which, with the definition (65) of η, yields

$$F(z) = B(\varepsilon)\left(\frac{T}{D}\right)^{1/2}\mathrm{e}^{-\frac{V(z+aZ)}{D}}. \tag{67}$$

As before, it might have been expected that $F(z)$ would be one of the time-independent solutions of Equation (15); namely, either a multiple of $\mathrm{e}^{-Vz/D}$ (as has just been found) or such a multiple plus a simple constant, but similar arguments by themselves could never deduce what multiple might arise. With the values (60) for $B(\varepsilon)$ and a, and the value (38) for D, the multiple turns out to be as follows:

$$F(z) = C(\varepsilon)\left(\frac{T}{D}\right)^{1/2}\mathrm{e}^{-Vz/D} = C(\varepsilon)\frac{T}{Z}6^{1/2}\,\mathrm{e}^{-6\varepsilon x}, \tag{68}$$

where the factor

$$C(\varepsilon) = (1 + 1{\cdot}6\varepsilon)\,\mathrm{e}^{-2\varepsilon} \tag{69}$$

varies rather little from 1 for small values of ε. Equation (68) shows indeed that it is droplets with extremely small values of $\varepsilon = VT/Z$ which can abound at relatively large nondimensional heights $x = z/Z$.

In terms of $S(V)$, the distribution of droplet production rate with respect to droplet terminal velocity, Equations (62) and (68) imply that the volume distribution of droplets at height z is close to

$$\left(\frac{T}{D}\right)^{1/2}\int_0^\infty S(V)\,\mathrm{e}^{-Vz/D}\,\mathrm{d}V. \tag{70}$$

Thus, it is a simple multiple of the Laplace transform of $S(V)$.

This section is now concluded with an initial attempt to look beyond that special case (16) which has been treated at such length. A simple step towards generalisation, might permit g to be a smooth, but otherwise rather general, even function of ζ with variance G . Then $f(z,t)$ would be a smooth function of z, still more likely to be well represented asymptotically by a solution of the partial differential equation (15). Also, that equation, in the case $V = 0$, would possess appropriate simple solutions of the general form (50).

When T remains unchanged, but parameters (such as Z) used to define the gust function are generalised, it may for $V = 0$ seem natural to use Equation (50) with a new shift of origin A replacing the existing shift aZ. Here, A should be determined from a revised boundary condition

$$f = A\frac{\partial f}{\partial z} \quad \text{on} \quad z = 0, \tag{71}$$

inferred from the true boundary condition by a generalisation of the argument in Equations (51) to (54).

If $g(\zeta)$ differs from zero only in the interval $-Z < \zeta < Z$, then Equation (52) needs replacement by an equation

$$TD\left(\frac{\partial f}{\partial z}\right)_{z=0} = \int_0^Z f(z,t)\,\mathrm{d}z\int_z^Z g(\zeta)\,\mathrm{d}\zeta. \tag{72}$$

Here, both sides represent the total diffusive transport into the surface $z = 0$ during a single time of flight T; the right-hand inner integral being the chance of a droplet initially at height $z < Z$ reaching $z = 0$ during that time (it might naturally have been expressed as an integral from $-Z$ to $-z$, which, however, is the same for an even function g as the integral from z to Z). Now the whole right-hand side, with reversed order of integration and $f(z, t)$ approximated by two terms of a Taylor series, becomes

$$\int_0^Z g(\zeta)\,\mathrm{d}\zeta \int_0^\zeta \left[f(0,t) + z\left(\frac{\partial f}{\partial z}\right)_{z=0} \right] \mathrm{d}z, \tag{73}$$

which, with expression (15) for D on the left-hand side, gives

$$\tfrac{1}{2}G\left(\frac{\partial f}{\partial z}\right)_{z=0} = Jf(0,t) + \tfrac{1}{4}G\left(\frac{\partial f}{\partial z}\right)_{z=0} \quad \text{where } J = \int_0^Z \zeta g(\zeta)\,\mathrm{d}\zeta \tag{74}$$

is the gust function's one-sided moment. Finally, this yields the boundary condition (67) with

$$A = \frac{G}{4J}. \tag{75}$$

In Sections 3 and 4, exact solutions of the integro-difference equation for a particular case were found to be well represented asymptotically by the solution (50) of the partial differential equation, and the boundary condition (51) which this solution asymptotically satisfies was then interpreted in terms of diffusive transport into the surface. In the present more general case, a boundary condition (71) can be thus interpreted if A takes the value (75); therefore, it may be reasonable to use the corresponding solution of the partial differential equation,

$$f(z,t) = \left(\frac{T}{\pi t}\right)^{1/2} \frac{z+A}{2Dt}\,\mathrm{e}^{-\frac{(z+A)^2}{4Dt}}, \tag{76}$$

as an asymptotic representation of $f(z, t)$. (Incidentally, the ratio of the general value (75) for A to the gust function's standard deviation $\sigma = G^{1/2}$ is not critically dependent on the exact form of that function; for example, the 'top-hat' form (16) with variance (17) makes $A = aZ$ with $a = \frac{1}{3}$ so that A/σ takes the value $3^{-1/2} = 0{\cdot}577$, while a Gaussian form gives A/σ the value $(\pi/8)^{1/2} = 0{\cdot}627$, and a rigorous minimum value of A/σ for any $g(\zeta)$ distribution is $0{\cdot}500$.)

By analogy to this solution (76) for $V = 0$, an exact solution of Equation (15) for $V > 0$ may be written

$$f(z,t) = B\left(\frac{T}{\pi t}\right)^{1/2} \frac{z+A}{2Dt}\,\mathrm{e}^{-\frac{(z+Vt+A)^2}{4Dt}}, \tag{77}$$

where the multiplying factor B becomes 1 when $V = 0$. Then we may evaluate the integral (61) for $F(z)$, using substitutions (63) and (65) with A replacing aZ, to give

$$F(z) = B\left(\frac{T}{D}\right)^{1/2} \mathrm{e}^{-\frac{V(z+A)}{D}} = C\left(\frac{T}{D}\right)^{1/2} \mathrm{e}^{-\frac{Vz}{D}} \tag{78}$$

with $C = B\,\mathrm{e}^{-VA/D}$, and it may be conjectured that (as before) C will differ rather little from 1 for small values of the terminal velocity V. In that case the overall conclusion (70) is unchanged.

6. Tentative further steps, taking droplet evaporation into account

The initial steps towards generalisation made in Section 5 were based firmly on results obtained in a particular case where exact solutions of the integro-difference equation could be asymptotically represented by exact solutions of the partial differential equation. Now a more tentative further generalisation is attempted in cases when, because appropriate exact solutions are unavailable, it may be necessary to proceed mainly by plausible analogy with the former case. These are cases when evaporation of droplets is taken into account.

Evaporation gradually reduces the radius of a droplet, so that its terminal velocity V also decreases. Here the dependence of V on radius is a familiar function which for small radius ($< 30\,\mu m$) varies as its square (Stokes-flow regime) while increasing more slowly for larger radii. Also, for given wind conditions (principally, relative humidity) the rate of reduction of radius is a certain (somewhat gradually decreasing) function of radius, and of V (which are themselves closely related), and it follows that the rate E at which the droplet fall speed V is reduced by evaporation can be specified as a function of V,

$$\frac{\mathrm{d}V}{\mathrm{d}t} = -E(V). \tag{79}$$

For a droplet whose terminal velocity V decreases in this way after it leaves the surface when $t = 0$, its net downward motion after time t, relative to that parcel of air in which it is situated, becomes

$$X = \int_0^t V\,\mathrm{d}t, \tag{80}$$

and it may appear plausible to use X in place of Vt in the former asymptotic solution (77), which would then become

$$f(z,t) = B\left(\frac{T}{\pi t}\right)^{1/2} \frac{z+A}{2Dt}\,\mathrm{e}^{-\frac{(z+X+A)^2}{4Dt}}. \tag{81}$$

As noted in relation to Equation (58), this involves a simple shift (from z to $z + X$) within the exponent to allow for downward displacement of the droplet by a distance X relative to an air particle; while, asymptotically, leaving the boundary condition (71) unchanged.

In general, however, expression (81) is no longer an exact solution of equation (15) – whose right-hand side it equates to

$$B\left(\frac{T}{\pi t}\right)^{1/2} \frac{1}{2Dt}\,\mathrm{e}^{-\frac{(z+X+A)^2}{4Dt}} \left[-\frac{3(z+A)}{2t} + \frac{(z+A)(z+X+A)^2}{4Dt^2} - \frac{X}{t}\right], \tag{82}$$

while its left-hand side takes the same form with $\mathrm{d}X/\mathrm{d}t = V$ replacing X/t at the end of the square brackets. Thus, they exactly coincide only when V is constant; on the other hand, the difference between them may plausibly be considered slight enough for expression (81) to be

regarded as a useful approximate solution of Equation (15). Then this expression may, for a drop where V takes the value V_0 when it leaves the surface at time $t = 0$, be used along with two integral relationships,

$$t = \int_V^{V_0} \frac{\mathrm{d}V}{E(V)} \quad \text{and} \quad X = \int_V^{V_0} \frac{V\,\mathrm{d}V}{E(V)}, \tag{83}$$

between t, X on the one hand and V_0, V on the other.

In terms of $S(V)$, the source function introduced in Equation (62) and an associated discussion, it is now $S(V_0)\,\mathrm{d}V_0$ which represents the rate of production per unit area per unit time of droplets which initially have terminal velocities between V_0 and $V_0 + \mathrm{d}V_0$. Moreover, a spray distribution function $s(z, V)$ may be defined so that the volume distribution at height z of droplets with terminal velocities between V and $V + \mathrm{d}V$ is $s(z, V)\,\mathrm{d}V$.

The approximate form (81) of $f(z, t)$, the probability distribution for the height z of a spray droplet at time t after it leaves the surface, may be used in a simple integral relationship

$$s(z, V) = \frac{1}{E(V)} \int_0^{\infty} S(V_0)\, f(z, t)\,\mathrm{d}V_0 \tag{84}$$

between $s(z, V)$ and $S(V_0)$; provided that t and X, where they appear in Equation (81) for $f(z, t)$, are expressed in terms of V_0 and V by equations (83). In equation (84), the multiplying factor

$$\frac{1}{E(V)} = \left| \frac{\mathrm{d}t}{\mathrm{d}V} \right| \tag{85}$$

is needed because $[S(V_0)\,\mathrm{d}V_0]\,\mathrm{d}t$ represents droplet production per unit area in a time interval $\mathrm{d}t$ while $s(z, V)\,\mathrm{d}V$ is the droplet distribution per unit volume in a fall-speed interval $\mathrm{d}V$.

Evidently, the exponential expression (81) for f lends itself to approximate evaluation of the integral (84) by the method of steepest descents. As a function of V_0, the exponent

$$\frac{(z + X + A)^2}{4Dt} \tag{86}$$

is a minimum where its first derivative

$$\frac{V_0}{E(V_0)} \frac{z + X + A}{2Dt} - \frac{1}{E(V_0)} \frac{(z + X + A)^2}{4Dt^2} \tag{87}$$

is equal to zero, giving

$$z + X + A = 2V_0 t; \tag{88}$$

in which case the exponent's second derivative with respect to V_0 is readily calculated as the positive quantity

$$\kappa = \frac{V_0}{E(V_0)D} \left[1 + \frac{V_0}{2t\,E(V_0)} \right]. \tag{89}$$

The method of steepest descents then approximates Equation (84) as

$$s(z, V) = \frac{1}{E(V)} S(V_0) f(z, t) \left(\frac{2\pi}{\kappa}\right)^{1/2}, \tag{90}$$

with t and X expressed in terms of V_0 and V by Equations (83) and with V_0 then expressed in terms of z and V by the minimum-exponent condition (88).

Special interest is, of course, attached to this condition (88), which statistically identifies the initial fall speed V_0 of those droplets which at height z, through evaporation, have predominantly acquired fall speed V. The condition appears to be a nontrivial conclusion from the line of argument presented in this paper.

7. Numerical results for the particular case of constant E

In the space that remains detailed calculations are presented for just one particular, relatively simple, case when the function $E(V)$ takes a constant value. These results are used to show in broad terms the contrast between spray calculations with and without evaporation – while their relevance to real ocean-spray processes is assessed briefly in the concluding Section 8 (where E is found to differ from a constant only moderately for relatively small droplets having radii $< 150\,\mu m$).

With constant E, Equations (83) give

$$Et = V_0 - V, \quad 2EX = V_0^2 - V^2, \tag{91}$$

so that the condition (88) linking V and V_0 becomes a quadratic equation

$$2E(z + A) = 3V_0^2 - 4VV_0 + V^2 \tag{92}$$

and V/V_0 can be expressed, in terms of a nondimensional variable

$$2E(z + A)V_0^{-2} = \alpha, \quad \text{as} \quad V/V_0 = 2 - (1 + \alpha)^{1/2}. \tag{93}$$

Figure 10 depicts how V/V_0 is reduced as the measure of height α rises; note that, on the steepest-descents approximation, droplets with initial fall speed V_0 have evaporated completely (since $V = 0$) where $\alpha = 3$. At the same time their number distribution has decayed with height somewhat less steeply than was suggested for cases without evaporation by equation (78) – just because of the diminution in terminal velocity V as z increases.

Indeed the number density for all spray droplets at height z may be written as an integral

$$s_0(z) = \int_0^\infty s(z, V)\, \mathrm{d}V \tag{94}$$

with respect to V; which, moreover, can be reformulated as an integral with respect to V_0 by use of the relation (92) between V and V_0. With Equation (90) for $s(z, V)$, this gives

$$s_0(z) = B \left(\frac{T}{D}\right)^{1/2} \int_0^\infty S(V_0) P(\alpha)\, \mathrm{e}^{-Q(\alpha)V_0(z+A)/D}\, \mathrm{d}V_0, \tag{95}$$

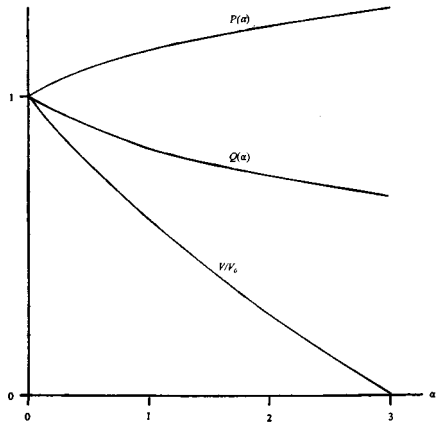

Figure 10. Dependence of V/V_0, $P(\alpha)$ and $Q(\alpha)$ on α.

where the nondimensional expressions

$$Q(\alpha) = 2\alpha^{-1}\left[(1+\alpha)^{1/2} - 1\right],$$

$$P(\alpha) = \tfrac{1}{2}\left[1 + (1+\alpha)^{-1/2}\right]\left[2(1+\alpha)^{1/2} - 1\right]^{1/2} \tag{96}$$

are also plotted in Figure 10. With no evaporation, $\alpha = 0$ so that $Q(\alpha) = P(\alpha) = 1$ and Equation (95) agrees precisely with the results of Section 5. (Unexpectedly, agreement is exact because the integral expression (66) in the case without evaporation has an unusual property; namely, that estimation by steepest descents gives its accurate value.) On the other hand, $Q(\alpha) < 1$ for positive α so that the reduction in number density with height z for droplets of initial fall speed V_0 becomes more gradual than a simple exponential $\exp(-V_0 z/D)$; the presence of the multiplier $P(\alpha)$ making little difference to this conclusion.

In broad terms, then, droplet number density decays more gradually, while droplet size is diminished, as a result of evaporation. Figure 10 quantifies both processes in the case of constant E analysed in this section.

8. General discussion

The paper ends with a general discussion which, while reviewing many obvious limitations on the value of analyses presented above, aims to derive from them as much insight as possible into ocean spray clouds at extreme wind speeds and their effect on TC thermodynamics. First, cloud physics data are used (i) to estimate droplet sizes for which the constant-E approximation of Section 7 may be valuable, (ii) to assess qualitatively how the conclusions will change for other droplet sizes, and (iii) to study implications for sea-air temperature differences. Next, careful consideration is given to questions of how analyses using a constant value of the Lagrangian correlation time can help to suggest conclusions relevant to ocean spray clouds situated within a turbulent boundary layer characterized in the classical manner. The discussion is then concluded with a forward look towards needs for future research.

Equation (79) for $E(V)$ allows it to be written as a product

$$E(V) = \left(-\frac{\mathrm{d}r}{\mathrm{d}t}\right)\left(\frac{\mathrm{d}V}{\mathrm{d}r}\right) \tag{97}$$

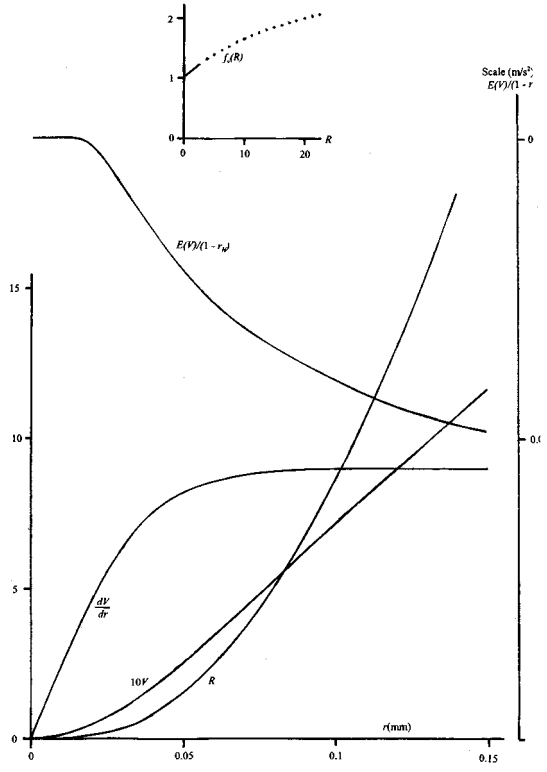

Figure 11. The bottom diagram shows a smooth curve $V(r)$, consistent with measurements of fall speed (in m/s) for droplets of radius r (in mm), together with its derivative $\mathrm{d}V/\mathrm{d}r$ and the associated Reynolds number R. The top diagram represents [16] the ventilation factor $f_v(R)$ by a solid straight line and a dotted parabola. In between, the value of $E/(1-r_H)$, as inferred from Equations (97) and (104), is plotted (in m/s^2; see right-hand scale) against r (in mm).

of the rate of decrease of droplet radius by evaporation and the slope of the graph of terminal velocity against radius. In Figure 11 a smooth curve consistent with the many good measurements of $V(r)$ is plotted together with its gradient $\mathrm{d}V/\mathrm{d}r$ and the associated Reynolds number $R = 2rV/\upsilon$. Here, the kinematic viscocity υ is taken as a datum value 16·6mm^2/s for typical TC winds at 25°C and 950mb. These are also the ambient conditions assumed for the $(-\mathrm{d}r/\mathrm{d}t)$ values derived as follows.

Rate of evaporation depends on the air's relative humidity

$$r_H = q_a/q_s(T_a), \tag{98}$$

defined as the ratio of water-vapour concentration by mass to its saturation value at the air temperature T_a. Actually, an evaporating droplet in moving air acquires almost instantly the wet-bulb temperature T_w such that

$$c_p(T_a - T_w) = L_v\left[q_s(T_w) - q_a\right]. \tag{99}$$

Equation (99) allows sensible-heat transfer (with specific heat c_p) from airstream to droplet to balance transfer of latent heat L_v from droplet to air – and is of such a simple form because quantitatively identical diffusion mechanisms (both molecular and turbulent) mediate each

Table 2.

r_H	0·75	0·80	0·85	0·90	0·95
T_w	21·64°	22·35°	23·04°	23·71°	24·36°
Ratio (100)	0·267	0·264	0·260	0·257	0·254

transfer. That equation yields, for the air temperature $T_a = 25°\text{C}$ assumed here, the values of T_w shown for different relative humidities r_H in Table 2 along with values of the ratio

$$\frac{q_s(T_w) - q_a}{q_s(T_a) - q_a} = \frac{q_s(T_w) - q_a}{(1 - r_H) q_s(T_a)}. \tag{100}$$

To simplify later results, this ratio is henceforth taken as 0·261 (close to all values in Table 2); which for $T_a = 25°$, with $q_s(T_a) = 0{\cdot}0207$, gives the value

$$q_s(T_w) - q_a = 0{\cdot}0054(1 - r_H) \tag{101}$$

for the vapour-concentration difference which drives droplet evaporation.

The rate $(-4\pi r^2\, \mathrm{d}r/\mathrm{d}t)\rho_L$ at which an evaporating droplet of density ρ_L (L for liquid water) would lose mass by pure molecular diffusion of vapour with diffusivity D_v takes a theoretical value

$$4\pi r D_v \rho_a \left[q_s(T_w) - q_a\right], \tag{102}$$

resulting from the fact that a steadily diffusing vapour concentration q must be a spherically symmetrical solution of Laplace's equation. Furthermore, experimental data on evaporation by a combination of diffusion with convection in a flow with Reynolds number R are conventionally expressed [16] in terms of a 'ventilation factor' $f_v(R)$ by which the theoretical value (102) needs to be multiplied, to give

$$\left(-\frac{\mathrm{d}r}{\mathrm{d}t}\right) = \frac{1}{r}\frac{\rho_a}{\rho_L} D_v \left[q_s(T_w) - q_a\right] f_v(R). \tag{103}$$

Here, f_v is expected to be close to 1 in the limit $R \to 0$ for very small drops, and the fact (see Figure 11) that these have $\mathrm{d}V/\mathrm{d}r$ proportional to r gives a clear indication why the product (97) for E is initially constant.

On the other hand, as V increases to 1 m/s (corresponding to $r = 0{\cdot}13\text{mm}$ and $R = 16$), the value of E falls by nearly a factor of 2. Undoubtedly, evaporation experiments are difficult; nonetheless, there is a present consensus in favour of $f_v(R)$ values as shown in an inset graph on Figure 11. Also, with $\rho_a D_v/\rho_L = 0{\cdot}031\text{mm}^2/\text{s}$ for $T_a = 25°\text{C}$, Equations (101 and (103) give

$$\left(-\frac{\mathrm{d}r}{\mathrm{d}t}\right) = \frac{f_v(R)}{r}(1 - r_H)(0{\cdot}000167\,\text{mm}^2/\text{s}), \tag{104}$$

leading, with Equation (97), to the values of $E/(1 - r_H)$ in m/s^2 plotted against r in Figure 11 and against V in Figure 12.

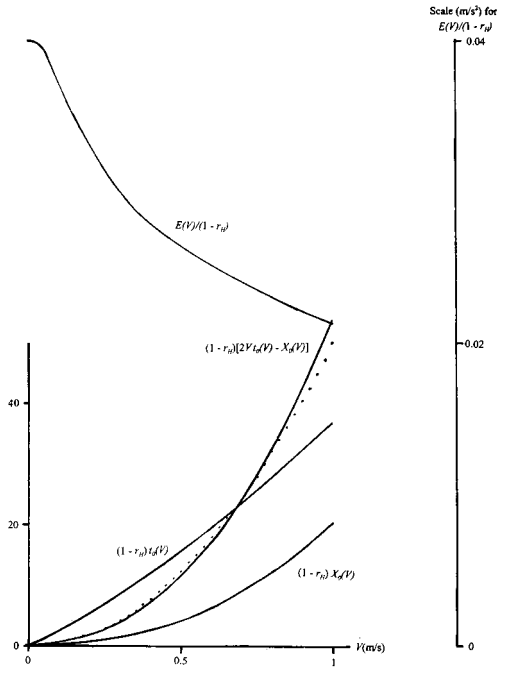

Figure 12. Values of $E(V)/(1-r_H)$ replotted (still in m/s^2; see right-hand scale) against V (in m/s), with (left-hand scale) the functions (106) and (109). Dotted line: the simple (constant-E) approximation $50V^2$ to expression (109).

Evidently, any constant-E approximation could at best be regarded as exceedingly crude in the fall-speed interval $0 < V < 1$ m/s, where $E/(1-r_H)$ falls from 0·040 to 0·021 m/s^2. Even so, the variation is by not more than a factor of 2 rather than by anything like a whole order of magnitude.

If in fact $E/(1-r_H)$ were crudely treated as approximately taking the constant value 0·03 m/s^2 in this interval, then Equation (93) could be used to specify the highest level z which droplets leaving the surface with fall speed V_0 could attain (corresponding to $\alpha = 3$) as satisfying

$$(1-r_H)(z+A) = 50V_0^2 \text{ metres}, \tag{105}$$

where V_0 is in m/s. Actually, this prediction can easily be assessed against a calculation avoiding the constant-E approximation.

Indeed, Figure 12 shows not only how $E(V)$ varies with V but also two other functions

$$t_0(V) = \int_0^V \frac{\mathrm{d}V}{E(V)}, \qquad X_0(V) = \int_0^V \frac{V\,\mathrm{d}V}{E(V)}, \tag{106}$$

in terms of which the relationship (88) between z, V and V_0 can be written

$$z + A = 2V_0\,[t_0(V_0) - t_0(V)] - [X_0(V_0) - X_0(V)]\,. \tag{107}$$

In particular, the height z at which, in a statistical sense, drops leaving the surface with fall speed V_0 have attained $V = 0$ (that is, have evaporated completely) satisfies

$$z + A = 2V_0 t_0(V_0) - X_0(V_0). \tag{108}$$

Accordingly, $(1 - r_H)(z + A)$ varies with V_0 like the function

$$(1 - r_H)\,[2Vt_0(V) - X_0(V)] \tag{109}$$

of V which also is plotted in the figure – together with a dotted line representing the very simple approximation (105). On the basis of this comparison, errors resulting from the constant-E approximation appear relatively modest. Even so, it may be desirable (and is indeed the author's intention) to repeat the whole analysis of Section 7 with the simple relationship (92) between V and V_0 replaced by its more accurate form (107).

In the meantime, a legitimate aim may be to draw from the constant-E analysis as many useful inferences as possible. These should include inferences relevant to TC thermodynamics, where the key problem is that the most detailed ocean-spray observations have been made only at wind speeds less than 28 m/s; therefore, an analyst's main goal should be to help in extrapolation to TC wind speeds of 50 to 60 m/s. Admittedly, an imperfect model can only yield imperfect predictions in any absolute sense; nonetheless, provided that it incorporates all essential physical effects acting on spray droplets (gusts, gravity, evaporation), it may be able to give some quantitative indication of how the extent, and the effects, of ocean spray will change when wind speed is doubled.

As to the extent of spray droplets of different sizes, the essential quantitative message of the constant-E analysis is that droplets generated at the surface have spatial distributions which are influenced by their initial size, as indicated from their fall speed V_0, in two opposing ways. On the one hand, evaporation gives their possible height z an absolute upper limit which Equation (105) specifies as as increasing with V_0 like V_0^2. On the other hand, at levels below this upper limit, gravity causes their distributions to decay exponentially as the height z increases, with an e-folding vertical distance of D/V_0 (or possibly up to 50% more if the $Q(\alpha)$ factor in Equation (95) is taken into account), which decreases like V_0^{-1} with increase of V_0.

There may perhaps be a suggestion here that, as D varies, vertical extent will be greatest for values of V_0 proportional to $D^{1/3}$ for which both spatial limitations are in balance. This would make droplets extend, typically, to heights varying as $D^{2/3}$; while, in the closely linear part of the (V, r) curve in Figure 11, their radii and volumes would vary respectively as $D^{1/3}$ and as D. The total mass of spray would then vary as $D^{5/3}$ for a given scale of source function $S(V_0)$ describing rate of production of droplets. Since on a conservative estimate (see below) D increases with at least the first power of the wind speed, such a suggestion implies that spray is augmented, in winds of doubled speed, by at least a factor of 3 over and above any effects of increased droplet production at this greater speed (which are themselves expected to be large). Clearly more research is needed on the soundness or otherwise of this inference; in the meantime, any implications that it may have for TC thermodynamics need to be outlined.

Here the crucial question (see Section 1) is whether or not inwardly spiralling and accelerating air, as it approaches the base of the eyewall before beginning its buoyancy-powered rise along a moist-air adiabat, starts that rise at a temperature significantly below the sea-surface temperature. Evidently, dense spray restricts severely any radiative component in sea-to-air transfer of sensible heat – which should therefore consist primarily of turbulent heat transfer with a transfer rate per unit horizontal area proportional to the product of wind speed and air-sea temperature difference. Such turbulent transfer has to balance those transfers of sensible heat from air to droplets which are described by Equation (99). In an equilibrium state, therefore, air-sea temperature difference is proportional to droplet evaporation rate (per

unit horizontal area) divided by wind speed. Accordingly, if the mass of spray per unit area encountered by the accelerating airstream varied only slowly, then as the relative humidity r_H approached 1 near the eyewall the droplet evaporation rate per unit area would approach zero and so too would the air-sea temperature difference.

The situation would be quite different, however, if a very steep increase in spray mass per unit area accompanied the accelerating wind's approach to the eyewall. Not only would this tend to counteract the $(1 - r_H)$ factor in the evaporation rate; more significantly, the heat balance processes could depart from equilibrium altogether, in that the last stages of saturation of an inwardly spiralling airstream, already cooler than the sea surface, would occur on its encounter with rather dense spray clouds. Then vertical gust components could rapidly initiate its buoyancy-powered moist-air ascent in the convective cloud of the eyewall – leaving no time for turbulent heat transfer to equilibrate its temperature with that of the sea surface. The implications for TC thermodynamics (see Section 1) would be substantial.

These considerations suggest why further studies of the influence of wind speed on spray distribution, including perhaps more detailed calculations using the present relatively simple model, may be valuable. Yet it is important also to bear in mind the model's limitations, and to compare it with models based on classical descriptions of the turbulent boundary layer.

The present model's most marked departure from such descriptions lies in its use of a constant value T for the Lagrangian correlation time. On the other hand, classical measurements in turbulent boundary layers do indicate an approximately constant variance for the vertical velocity component; so that, once T has been taken constant, the assumption of a constant variance G for vertical displacement in time T appears quite reasonable. Taken together, these assumptions lead to the constant value (15) for the diffusivity D; whereas a classical expression like

$$D = Ku_*z \tag{110}$$

(in terms of a friction velocity u_*, the Karman constant $K = 0{\cdot}4$ and the height z) corresponds rather to a Lagrangian correlation time increasing with height in proportion to z/u_* while G varies as z^2.

Admittedly, expected departures of the atmospheric boundary layer over deeply heaving seas from such classical behaviour may involve for smaller values of z some increased coherence of vertical motion, and this has been part of the motivation for the present constant-T model. Nonetheless it may be useful to ask if this model has anything in common with classical spray-distribution predictions.

Such a comparison can at least be made in the steady-state case with evaporation neglected, when Equation (110) for the diffusivity yields an equation

$$-V\frac{\partial f}{\partial z} = \frac{\partial}{\partial z}\left(Ku_*z\frac{\partial f}{\partial z}\right) \tag{111}$$

for the distribution of droplets with fall speed V. Briefly, it is solutions of equation (111) proportional to

$$z^{-V/Ku_*} \tag{112}$$

which correspond to the steady-state solutions (78) of the present paper; and which, like those, show a broadly analogous slow decrease with z when V is small compared with other parameters in the problem. By contrast, droplet evaporation cannot easily be allowed for within such

a steady-state theory – and this consideration tends to reinforce the need for research aimed at extending farther the approach outlined in Sections 6 and 7.

In such extensions, of course, it may be logical to employ a value of D equal to the average of expression (110) over the boundary layer thickness. This argument underlies the earlier suggestion that D should increase with at least the first power of the wind speed. Yet beyond any additional theoretical studies, the problem's biggest need is for real data on ocean spray distributions at extreme wind speeds, and the paper may be concluded with just a brief suggestion of how that might be achieved. For all-weather spray measurements in the North Sea, the HEXOS platform Meetpost Noordwijk has proved highly effective [2]. One or more similarly equipped fixed platforms are now needed in a sea area subject to extreme TC conditions such as the Gulf of Mexico; where, fortunately, suitable structures already exist in the form of oil rigs. Instrumentation of high quality, comparable to that used in HEXOS, with automatic logging, needs to be installed on well chosen rigs so that, even when forecasts of extreme winds necessitate crew evacuation, data about ocean spray in such conditions can still be recorded.

References

1. E. L. Andreas, J. B. Edson, E. C. Monahan, M. P. Rouault and S. D. Smith, The spray contribution to net evaporation from the sea: a review of recent progress. *Boundary Layer Meteorol*. 72 (1995) 3–52.
2. J. De Cosmo, K. B. Katsaros, S. D. Smith, R. J. Anderson, W. Oost, K. Bumke and H. Chadwick, Air-sea exchange of water vapor and sensible heat: the HEXOS results. *J. Geophys. Res*. 101 (1996) 12001–12016.
3. V. D. Pudov, The ocean response to the cyclones' influence and its possible role in their tracks. In: J. Lighthill, Zheng Zhemin, G. Holland and K. Emanuel (eds.) *Tropical Cyclone Disasters*. Beijing: Peking University Press (1993) pp. 367–376.
4. C. W. Fairall, J. D. Kepert and G. J. Holland, The effect of sea spray on surface energy transports over the ocean. *The Global Atmosphere and Ocean System* 2 (1994) 121–142.
5. J. Lighthill, Fluid Mechanics of Tropical Cyclones. *J. Theor. Comput. Fluid Dyn*. 10 (1998) 3–21.
6. K. A. Emanuel, The theory of hurricanes. *Ann. Rev. Fluid Mech*. 23 (1991) 179–196.
7. J. Lighthill, G. J. Holland, W. M. Gray, C. Landsea, K. Emanuel, G. Craig, J. Evans, Y. Kurihara and C. P. Guard, Global climate change and tropical cyclones. *Bull. Amer. Met. Soc*. 75 (1994) 2147–2157.
8. A. Henderson-Sellers, H. Zhang, G. Berz, K. Emanuel, W. Gray, C. Landsea, G. Holland, J. Lighthill, S. L. Shieh, P. Webster and K. McGuffie, Tropical cyclones and global climate change: A post-IPCC assessment. *Bull. Amer. Met. Soc*. 79 (1998) 19–38.
9. S. A. Petrichenko and V. D. Pudov, O parametrizatsii teplo- i vlago-obmena mezhdu okeanom i atmosferoi v tropikakh v shtormovykh usloviyakh. *Meteorologiya i Gidrologiya* (1996, No. 6) 92–100.
10. P. G. Black, G. J. Holland and V. Pudov, Observations of sea-air temperature difference in tropical cyclones as a function of wind speed: importance of spray evaporation. In: J.D. Jasper and P.J. Meighen (eds.) *Parametrisation of Physical Processes: Papers Presented at the Fifth BMRC Modelling Workshop, November 1993*. BMRC Research Report No. 46, Melbourne: Bureau of Meteorology Research Centre (1994) p. 87.
11. M. P. Rouault, P. G. Mestayer and R. Schiestel, A model of evaporating spray droplet dispersion. *J. Geophys. Res*. 96 (1991) 7181–7200.
12. J. B. Edson and C. W. Fairall, Spray droplet modeling. I. Lagrangian model simulation of the turbulent transport of evaporating droplets. *J. Geophys. Res*. 99 (1994) 25295–25311.
13. G. de Leeuw, Profiling of aerosol concentrations, particle size distributions and relative humidity over the North Sea. *Tellus* 42B (1990) 342–354.
14. G. I. Taylor, Diffusion by continuous movements. *Proc. Lond. Math. Soc*. (2) 20 (1921) 196–212.
15. J. C. R. Hunt, Turbulent diffusion from sources in complex flows. *Ann. Rev. Fluid Mech*. 17 (1985) 447–485.
16. H. R. Pruppacher and J. D. Klett, *Microphysics of Clouds and Precipitation*, 2nd edition. Dordrecht: Kluwer (1997) 954pp.